The Plant Cell, Vol. 30: 1617–1627, July 2018, www.plantcell.org © 2018 ASPB.

Loss of RNA-Directed DNA Methylation in Maize Chromomethylase and DDM1-Type Nucleosome Remodeler Mutants[OPEN]

Fang-Fang Fu,[a] R. Kelly Dawe,[a,b,1] and Jonathan I. Gent[a,1]

[a]Department of Plant Biology, University of Georgia, Athens, Georgia 30602
[b]Department of Genetics, University of Georgia, Athens, Georgia 30602

ORCID IDs: 0000-0002-3187-9308 (F.-F.F.); 0000-0003-3407-4553 (R.K.D.); 0000-0002-3584-7717 (J.I.G.)

Plants make use of distinct types of DNA methylation characterized by their DNA methyltransferases and modes of regulation. One type, RNA-directed DNA methylation (RdDM), is guided by small interfering RNAs (siRNAs) to the edges of transposons that are close to genes, areas called mCHH islands in maize (*Zea mays*). Another type, chromomethylation, is guided by histone H3 lysine 9 methylation to heterochromatin across the genome. We examined DNA methylation and small RNA expression in plant tissues that were mutant for both copies of the genes encoding chromomethylases as well as mutants for both copies of the genes encoding DECREASED DNA METHYLATION1 (DDM1)-type nucleosome remodelers, which facilitate chromomethylation. Both sets of double mutants were nonviable but produced embryos and endosperm. RdDM was severely compromised in the double mutant embryos, both in terms of DNA methylation and siRNAs. Loss of 24-nucleotide siRNA from mCHH islands was coupled with a gain of 21-, 22-, and 24-nucleotide siRNAs in heterochromatin. These results reveal a requirement for both chromomethylation and DDM1-type nucleosome remodeling for RdDM in mCHH islands, which we hypothesize is due to dilution of RdDM components across the genome when heterochromatin is compromised.

INTRODUCTION

Chromatin modification directed by RNA interference and related processes is essential to genome defense in most eukaryotes. The molecular mechanisms vary even within the same cell, but key features are small interfering RNAs (siRNAs), which guide argonaute proteins and induce methylation of histone H3 lysine 9 (H3K9me) (Holoch and Moazed, 2015). RNA-directed DNA methylation (RdDM) is a well-characterized example in plants (Cuerda-Gil and Slotkin, 2016). RdDM leads to H3K9me2 (Jackel et al., 2016; Fultz and Slotkin, 2017), but as its name suggests, is better known for methylating DNA. At least two *Arabidopsis thaliana* proteins that function in RdDM physically interact with a DNA methyltransferase, indicating a direct connection between RdDM and DNA methylation (Gao et al., 2010; Zhong et al., 2014). RdDM represses repetitive and foreign DNA but can also influence gene expression, at gene regulatory elements for example (Rowley et al., 2017), and is involved in epigenetic phenomena such as paramutation (Hollick, 2017) and genomic imprinting (Satyaki and Gehring, 2017).

DNA methylation occurs at cytosines in all sequence contexts and is catalyzed by three distinct types of methyltransferases in plants (Du et al., 2015). The first, related to Arabidopsis METHYLTRANSFERASE1 (MET1), which is homologous to mammalian DNA Methyltransferase 1 (DNMT1), is responsible for replication-coupled CG methylation. The second, related to Arabidopsis CHROMOMETHYLASE1 (CMT1), CMT2, and CMT3, methylates CHGs and CHHs, where H is A, T, or C. The chromodomains of these methyltransferases guide their activity to regions of H3K9me1 or H3K9me2. The third, related to Arabidopsis DOMAINS REARRANGED METHYLTRANSFERASE1 (DRM1) and DRM2, methylates cytosines in all sequence contexts through RdDM. Depending on the species, methylation in the CHH context (mCHH) can be used as an indicator of RdDM, as mCHH produced by CMT is of lesser magnitude than that of RdDM (Niederhuth et al., 2016). Division of methylation contexts into mCG, mCHG, and mCHH is a helpful simplification, but methyltransferases have additional nucleotide preferences (Gouil and Baulcombe, 2016).

Although RdDM was discovered as a mechanism that initiates methylation at previously unmethylated DNA (referred to as de novo methylation; Wassenegger et al., 1994), discoveries since then have revealed that most RdDM occurs at already-methylated and repressed loci (Cuerda-Gil and Slotkin, 2016). This maintenance form of RdDM, called canonical RdDM, depends on the activity of the RNA polymerase II variants Pol IV and Pol V and is responsible for the majority of 24-nucleotide siRNAs. Canonical RdDM in Arabidopsis relies on histone H3 lysine 9 methylation (H3K9me) and lysine 4 demethylation (Johnson et al., 2008, 2014; Kuhlmann and Mette, 2012; Greenberg et al., 2013; Law et al., 2013; Zhang et al., 2013; Blevins et al., 2014; Stroud et al., 2014; Li et al., 2015b). Canonical RdDM also requires DNA methylation, as *drm* and *cmt* mutants have reduced levels of 24-nucleotide siRNAs (Law et al., 2013; Stroud et al., 2014; Li et al., 2015b). DNA methylation may act indirectly by impacting the levels of H3K9me2, as histone methyltransferase mutants also lose 24-nucleotide siRNAs (Stroud et al., 2014). H3K9me2 recruits Pol IV (Law et al., 2013; Zhang et al., 2013), but DNA methylation also promotes RdDM through Pol V interacting factors (Johnson et al., 2014; Liu et al., 2014).

[1]Address correspondence to gent@uga.edu or kdawe@uga.edu.
The author responsible for distribution of materials integral to the findings presented in this article in accordance with the policy described in the Instructions for Authors (www.plantcell.org) is: Jonathan I. Gent (gent@uga.edu).
[OPEN]Articles can be viewed without a subscription.
www.plantcell.org/cgi/doi/10.1105/tpc.18.00053

IN A NUTSHELL

Background: DNA methylation is a chemical modification of DNA consisting of addition of a methyl group to cytosine nucleotides in the DNA molecule. There are three major forms of DNA methylation in vascular plants: (1) replication-coupled CG methylation, (2) chromomethylation, and (3) RNA-directed DNA methylation (RdDM). Chromomethylation is catalyzed by chromomethyltransferases (CMTs), directed by methylation of histone H3 lysine 9, and marks repressed repetitive DNA in heterochromatin. Heterochromatin depends in part on the nucleosome remodeling protein DDM1, which allows access of methyltransferases to nontranscribed, nucleosome-bound DNA. RdDM occurs at heterochromatin boundaries and depends on transcription and a form of RNAi.

Questions: Chromatin modifications associated with heterochromatin promote RdDM, yet heterochromatin itself inhibits RdDM. This apparent contradiction made us wonder what the relationship is between chromomethylatin and RdDM, and whether the relationship differs between maize, whose genome is filled with repetitive DNA, and Arabidopsis, whose genome has little repetitive DNA. In particular, we wondered what would happen to RdDM in *ddm1* and *cmt* mutants in maize.

Findings: We found that both *ddm1* and *cmt* mutants survive through endosperm and early embryo development but are nonviable. Whole-genome DNA methylation and small RNA sequencing of developing embryo and endosperm revealed dramatic loss of RdDM in mutants. Loss of 24-nucleotide small interfering RNA (siRNA) from heterochromatin boundaries was coupled with a gain of 21-, 22-, and 24-nucleotide siRNAs across the repetitive genome, although increased siRNAs were not correlated with increased DNA methylation. Taken together with discoveries from Arabidopsis and rice, we propose a model that when heterochromatin is compromised, RdDM components are scattered from heterochromatin boundaries across the large, repetitive maize genome such that they cannot act in concert for productive RdDM.

Next steps: We predict that any mutants that compromise heterochromatin will also lose RdDM. Currently unavailable but informative mutants in maize would be ones that are defective in histone H3 lysine methylation or in replication-coupled CG methylation.

The heterochromatic middle regions of long transposons are depleted of RdDM relative to their euchromatin-flanking ends (Lee et al., 2012; Zhong et al., 2012; Stroud et al., 2013, 2014; Zemach et al., 2013; Li et al., 2015b). Enrichment for RdDM at heterochromatin-euchromatin boundaries is especially clear in maize (*Zea mays*) because its heterochromatin and euchromatin are highly interspersed (Gent et al., 2013, 2014; Li et al., 2015a; Niederhuth et al., 2016). That heterochromatin inhibits RdDM is also suggested by activation of RdDM in normally heterochromatic regions in plants that lack the SNF2 family nucleosome remodeling protein DECREASED DNA METHYLATION1 (DDM1) (Nuthikattu et al., 2013; Stroud et al., 2013; Creasey et al., 2014; McCue et al., 2015; Panda et al., 2016), known as LYMPHOID SPECIFIC HELICASE in mammals (Dennis et al., 2001). DDM1 is required for access of MET1 and CMT-type methyltransferases to nontranscribed, nucleosome-bound DNA in Arabidopsis (Lyons and Zilberman, 2017). In its absence, mCG, mCHG, and H3K9me2 are reduced and chromocenters partially decondensed (Gendrel et al., 2002; Soppe et al., 2002).

The vegetative cell of pollen in Arabidopsis provides another line of evidence that heterochromatin inhibits RdDM because this cell type undergoes a dramatic decondensation of heterochromatin coupled with activation of RdDM (Schoft et al., 2009; Slotkin et al., 2009; Mérai et al., 2014). DDM1 may be reduced or absent from vegetative cells, as transgene-driven expression of a DDM1 fusion protein from a *ddm1* promoter produced signal in sperm but not in vegetative cells (Slotkin et al., 2009). Vegetative cells have increased mCHH (Calarco et al., 2012; Ibarra et al., 2012) primarily driven by CMT2, but also by DRM2 activity (Hsieh et al., 2016). The apparent contradiction between chromatin modifications associated with heterochromatin promoting RdDM, yet heterochromatin itself inhibiting RdDM may be explained by the relative abundance of chromatin modifications (e.g., by the ratio of H3K9me1 to H3K9me2; Stroud et al., 2014), and by higher-order chromatin structure that affects chromatin accessibility to RNA polymerases.

Its quick life cycle, small genome, and resilience to loss of DNA methylation have made Arabidopsis the plant model of choice for research on DNA methylation and chromatin. The discoveries made with Arabidopsis have been tremendously helpful in understanding similar phenomena plants that are more difficult to work with, such as maize, with its large, repetitive genome and nonviable methylation mutants (Li et al., 2015a). However, the differences between maize and Arabidopsis also limit the extent to which results can be projected from Arabidopsis to maize. Maize lacks a CMT2-type chromomethylase (Zemach et al., 2013; Bewick et al., 2017), has multiple copies of the major subunits of Pol IV and Pol V complexes with potential for specialized functions (Haag et al., 2014), has abundant meiotic phased siRNAs (Johnson et al., 2009; Zhai et al., 2015), and has abundant 22-nucleotide siRNAs (Nobuta et al., 2008; Wang et al., 2009).

The maize genome encodes two chromomethylases, named ZMET2 and ZMET5 (also known as DMT102 and DMT105) (Li et al., 2014). Both are functionally more similar to CMT3 than to CMT1 or CMT2 (Bewick et al., 2017). The maize genome also encodes two DDM1-like nucleosome remodelers, CHR101 and CHR106 (Li et al., 2014). The effects of single mutants of all four genes on whole genome methylation have been investigated previously (Gent et al., 2014; Li et al., 2014; Gouil and Baulcombe, 2016). Single mutants of *zmet2* and *zmet5* have reduced mCHG in both leaves and developing ears and reduced mCHH in leaves but not in developing ears. Single mutants of *chr101* have reduced

mCHH in leaves, and single mutants of *chr106* have reduced mCHH and mCHG in leaves (Li et al., 2014). Neither *chr101* nor *chr106* has been tested in developing ears. The effects of single mutants on siRNAs have not been reported, and it is not clear whether reduced RdDM explains their reduced mCHH.

Here, we investigated the relationships between RdDM and chromomethylases and DDM1-type nucleosome remodelers using mutants in maize. We found that double mutants of *chr101* and *chr106* and double mutants of *zmet2* and *zmet5*, while nonviable (Li et al., 2014), can produce embryos and endosperm. Analysis of DNA methylation and siRNAs in both tissues revealed that RdDM was severely compromised in developing embryos, with near complete loss of both 24-nucleotide siRNAs and mCHH from mCHH islands. The loss of 24-nucleotide siRNAs from mCHH islands was accompanied by dramatic gains of 21- and 22-nucleotide siRNAs at heterochromatic loci in the genome, but these siRNAs did not direct DNA methylation.

RESULTS

Generation of *ddm1* double and *cmt* Double Mutant Embryo and Endosperm

To make plants that lacked chromomethylases or DDM1-type nucleosome remodelers, we obtained UniformMu stocks with *Mu* insertions in exons of *Zmet2* (*mu1013094*) (Gent et al., 2014) and *Zmet5* (*mu1017456*), and in the DDM1-encoding genes *Chr101* (*mu1044815*) and *Chr106* (*mu1021319*) (Supplemental Table 1). Here, we will refer to *zmet2 zmet5* homozygous double mutants as *cmt*, and the *chr101* and *chr106* double mutants as *ddm1*. Mutants that carried a single wild-type copy of either *Zmet2* or *Zmet5* were viable and fertile, and crosses between such mutants produced kernels with sectors of pigmented aleurone (Supplemental Figure 1). This phenotype is characteristic of *Mutator* transposon activity in UniformMu stocks, where excision of a *Mu* from the *bz1-mum9* allele of the *Bz1* gene can restore pigmentation in small sectors during development (McCarty et al., 2005). *Mu* activation has been observed in a maize mutant lacking the RNA-directed RNA polymerase MEDIATOR OF PARAMUTATION1 (MOP1), which synthesizes the antisense strand of Pol IV transcripts (Woodhouse et al., 2006; Haag et al., 2014). We found a tight correlation between pigmented sectors in the aleurone and *zmet2 zmet5* (*cmt*) double mutant genotype (Supplemental Table 2). The *cmt* kernels contained both endosperm and embryos but were usually incapable of more than a couple centimeters of root development upon germination. A second pair of *zmet2* and *zmet5* alleles (*zmet2-m1* and *zmet5-m1*) that was introgressed into the B73 genetic background produced homozygous double mutant kernels at the expected ratios and were also nonviable (Supplemental Table 3). Failure to produce double mutant plants with these alleles was previously reported (Li et al., 2014). These kernels lacked the *Mu* insertion in the *Bz1* gene and so were incapable of pigmentation sectoring. Mutants that carried a single wild-type copy of either *Chr101* or *Chr106* were viable and fertile but produced homozygous double mutant (*ddm1*) kernels that were nonviable and had small embryos (Supplemental Table 2 and Supplemental Figure 1). Although in the *bz1-mum9* background, these *ddm1* kernels did not exhibit the sectoring phenotype of *cmt* mutants. They also did not germinate, not even to produce a root tip. A second set of *chr101* and *chr106* alleles (*chr101-m3* and *chr106-m1*) that was introgressed into B73 did not produce any homozygous double mutant kernels (Supplemental Table 3), consistent with the prior study (Li et al., 2014).

Loss of DNA Methylation Flanking Genes in *cmt* and *ddm1* Embryo and Endosperm

To determine the effects of the mutations on DNA methylation, we performed whole-genome bisulfite sequencing (WGBS) using the methylC-seq method (Urich et al., 2015) in three tissues: mature endosperm, developing endosperm 14 d after pollination (DAP), and 14-DAP embryos. In *cmt* mutants, mCHG was reduced to near background levels in all three tissues, with little or no effect on mCG (Figure 1). In *ddm1*, both mCHG and mCG were mildly reduced (40% reduction in mCG; 50% in mCHG in 14-DAP embryos). These effects on mCHG (nearly absent in *cmt*) and mCHG and mCG (reduced in *ddm1*) are consistent with the expected roles of chromomethylases and DDM1-like nucleosome remodelers in transcriptionally silent heterochromatin. Unexpectedly, we found that mCHH was nearly absent in *cmt* 14-DAP embryos, strongly reduced in mature endosperm, and slightly reduced in 14-DAP endosperm (Figure 1). The effect on mCHH was not due to a linked background mutation in the UniformMu-derived *cmt* mutant, as 14-DAP sibling embryos with a single wild-type copy of either *Zmet2* or *Zmet5* had near wild-type levels of mCHH (Supplemental Figure 2). mCHH was reduced in *ddm1* embryos and endosperm, particularly in mature endosperm (Figure 1). The effect of *ddm1* on RdDM is more evident when considered in the light of the fact that ZMET2 and ZMET5 can methylate CHH, particularly in the CAA and CTA contexts (Gouil and Baulcombe, 2016). The mCCH subset of mCHH is more specific to RdDM. The *ddm1* mutant had a strong effect on mCCH and less of an effect on mCHH in 14-DAP embryos (Figure 1). A single wild-type copy of either *Chr101* or *Chr106* largely restored mCHH in mature endosperm, indicating that the loss of RdDM in *ddm1* was not due to a background mutation linked to either gene (Supplemental Figure 3).

In developing ear, mCHH is greatly reduced in *mop1* mutants lacking the RNA-directed RNA polymerase MOP1, which is coupled with Pol IV in synthesis of 24-nucleotide siRNAs (Gent et al., 2014; Haag et al., 2014; Li et al., 2015a). *Mop1* is highly expressed in reproductive tissue, in embryo, and in endosperm (Sekhon et al., 2011). We performed WGBS on *mop1-1* mature endosperm and found ~50% reduction in mCHH flanking genes, indicating MOP1 function in endosperm, though probably not as the only source of antisense RNA in RdDM (Figure 1D). This experiment also revealed a high level of variation in mCHH in mature endosperm, as the wild-type *Mop1* siblings (B73-related) had methylation levels nearly twice as high as the wild-type mature endosperm in Figure 1C and slightly higher than the *ddm1* heterozygote mature endosperm (W22-related) (Supplemental Figure 3).

Loss of 24-Nucleotide siRNAs in *cmt* and *ddm1* Developing Embryo and Endosperm

Since 24-nucleotide siRNAs guide argonautes in RdDM, we sequenced small RNA from 14-DAP endosperm and embryo.

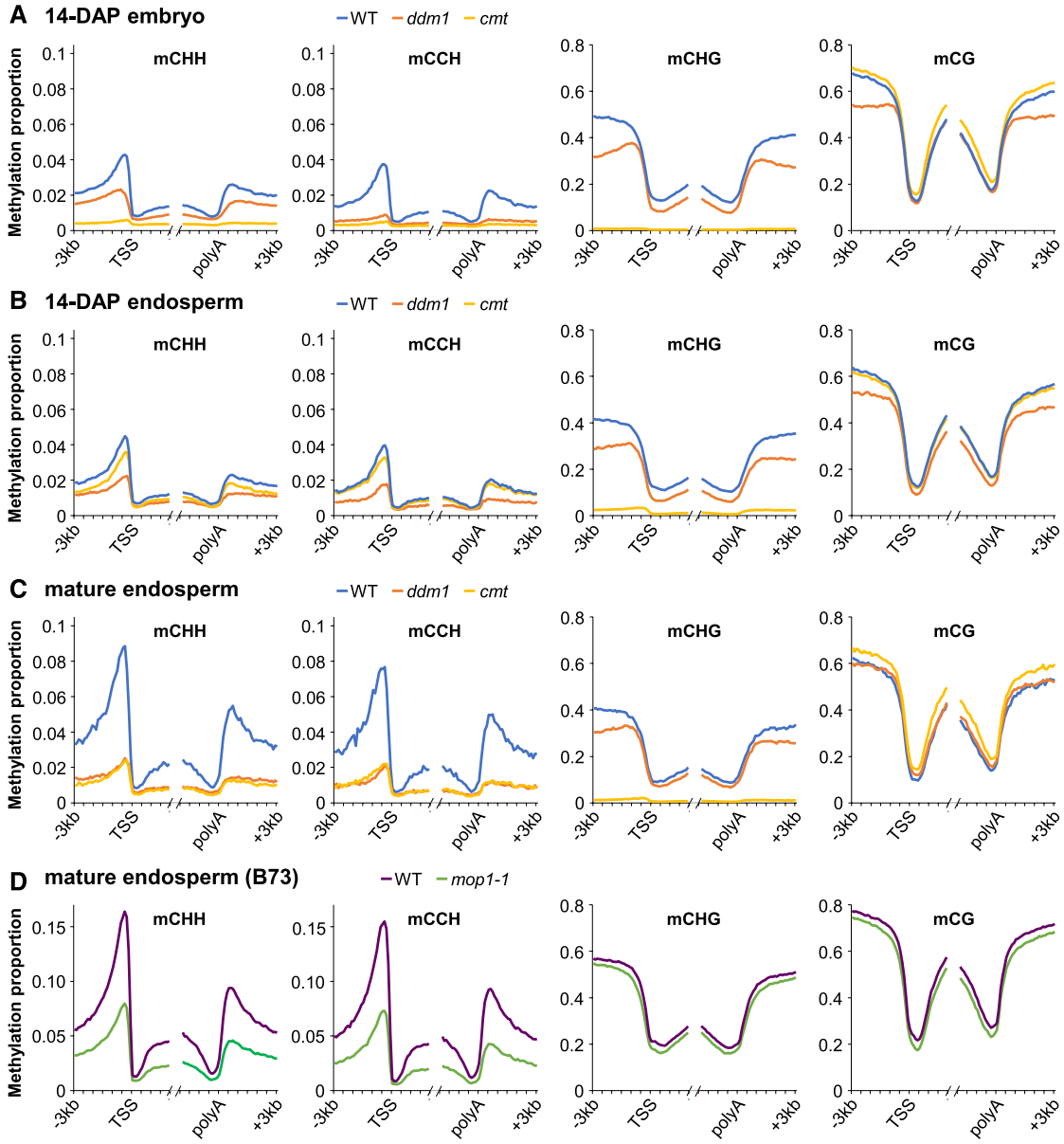

Figure 1. DNA Methylation Profiles Near Genes in Double Mutants.

(A) Methylation in 14-DAP embryo. All genes were defined by their annotated transcription start sites (TSS) and polyadenylation sites (polyA) and split into nonoverlapping 100-bp intervals. Methylation for each sample was calculated as the proportion of methylated C over total C in each sequence context (CHH, CCH, CHG, and CG) averaged for each 100-bp interval.
(B) Methylation in 14-DAP endosperm, as in **(A)**.
(C) Methylation in mature endosperm, as in **(A)**.
(D) Methylation in mature B73 endosperm, as in **(A)**. The wild type was derived from *Mop1* homozygous siblings of the *mop1-1* mutants.

To quantify siRNA abundance, we normalized siRNA counts by microRNA (miRNA) counts. We included all mappable small RNAs, both uniquely mapping and multimapping. There was a nearly complete loss of 24-nucleotide siRNAs from gene flanks in both *cmt* and *ddm1* 14-DAP embryos and a partial loss in 14-DAP endosperm (Figure 2A). Analysis of the uniquely mapping subset of siRNAs showed similar trends and revealed a >50% decrease in the proportion of uniquely mapping siRNAs in *ddm1* and in *cmt* embryos (Figures 2B and 2C). Loss of 24-nucleotide siRNAs was also evident from the distribution of total siRNA lengths: In homozygous wild-type individuals and heterozygous mutants, the dominant siRNA length was 24 nucleotides, but in *cmt* and *ddm1*, it shifted to 22 nucleotides and to a lesser extent 21 nucleotides (Figure 2D). DNA transposons with terminal inverted repeats of the

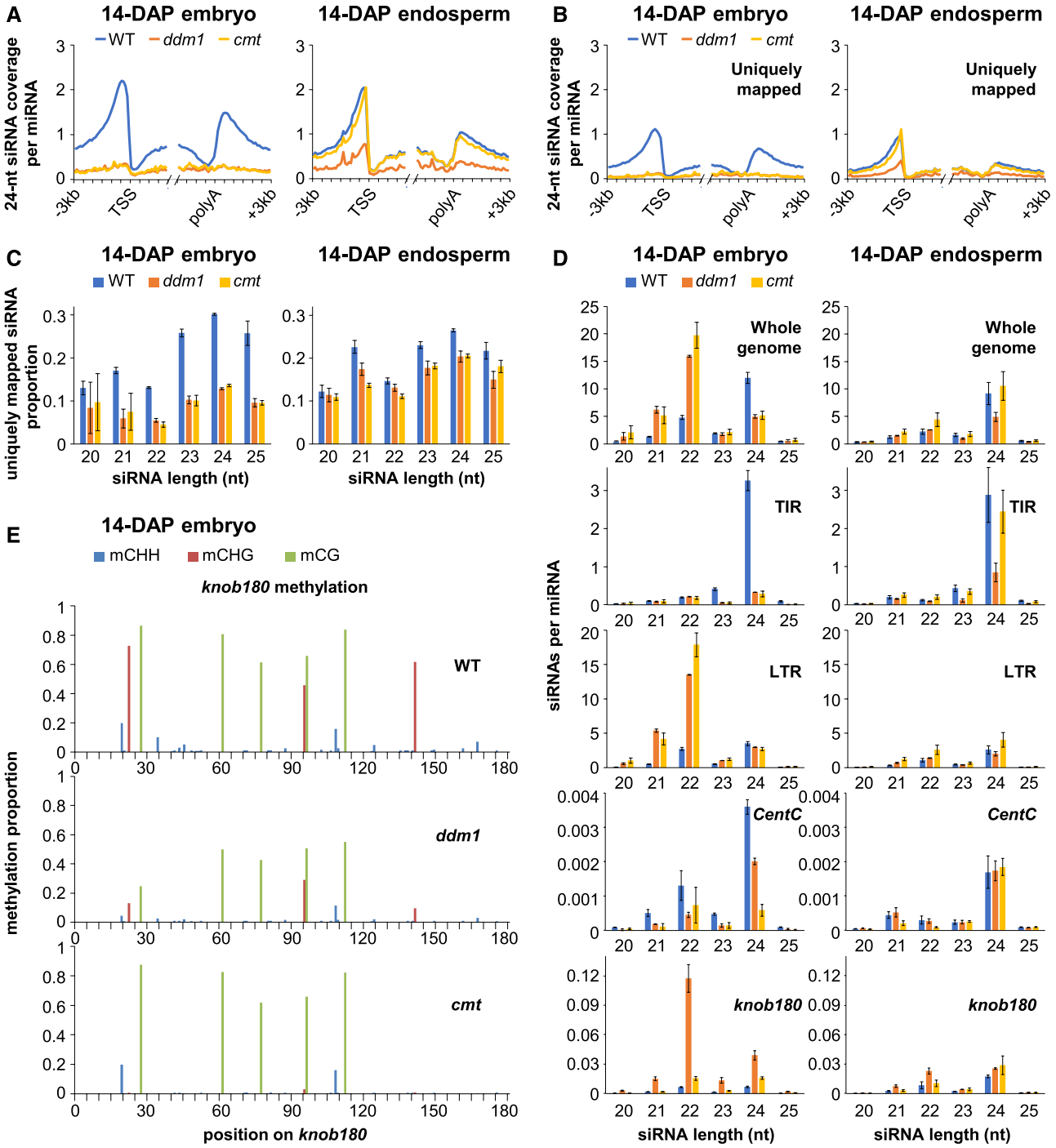

Figure 2. Loss of 24-Nucleotide siRNAs and Gain of 21- and 22-Nucleotide siRNAs in Double Mutants.

(A) The 24-nucleotide siRNA coverage near genes. All genes were defined by their annotated transcription start sites (TSS) and polyadenylation sites (polyA) and split into nonoverlapping 100-bp intervals. The siRNA coverage for each 100-bp interval was summed for the complete set of genes and normalized by miRNAs.

(B) Uniquely mapped 24-nucleotide siRNA coverage near genes, as in **(A)**.

(C) Proportion of uniquely mapped siRNAs for each length.

(D) Length distribution of various classes of siRNAs. "Whole genome" includes all mapped siRNAs. "TIR" includes all siRNAs that overlapped by at least half their lengths to *Mutator*, *hAT*, *Harbinger*, or *Mariner* TIR transposons. "LTR" includes all siRNAs that overlapped by at least half their lengths with *Gypsy* or *Copia* LTR retrotransposons. *CentC* includes all siRNAs that aligned to a *CentC* consensus sequence and *knob180* includes all siRNAs that aligned to a *knob180* consensus sequence. siRNA counts were normalized per miRNA. Error bars are standard errors of the means for the biological replicates of each genotype.

(E) Single-base-pair DNA methylation in *knob180* repeats. WGBS reads were mapped to the *knob180* consensus sequence and methylation calculated as the proportion of methylated C over total C in each sequence context.

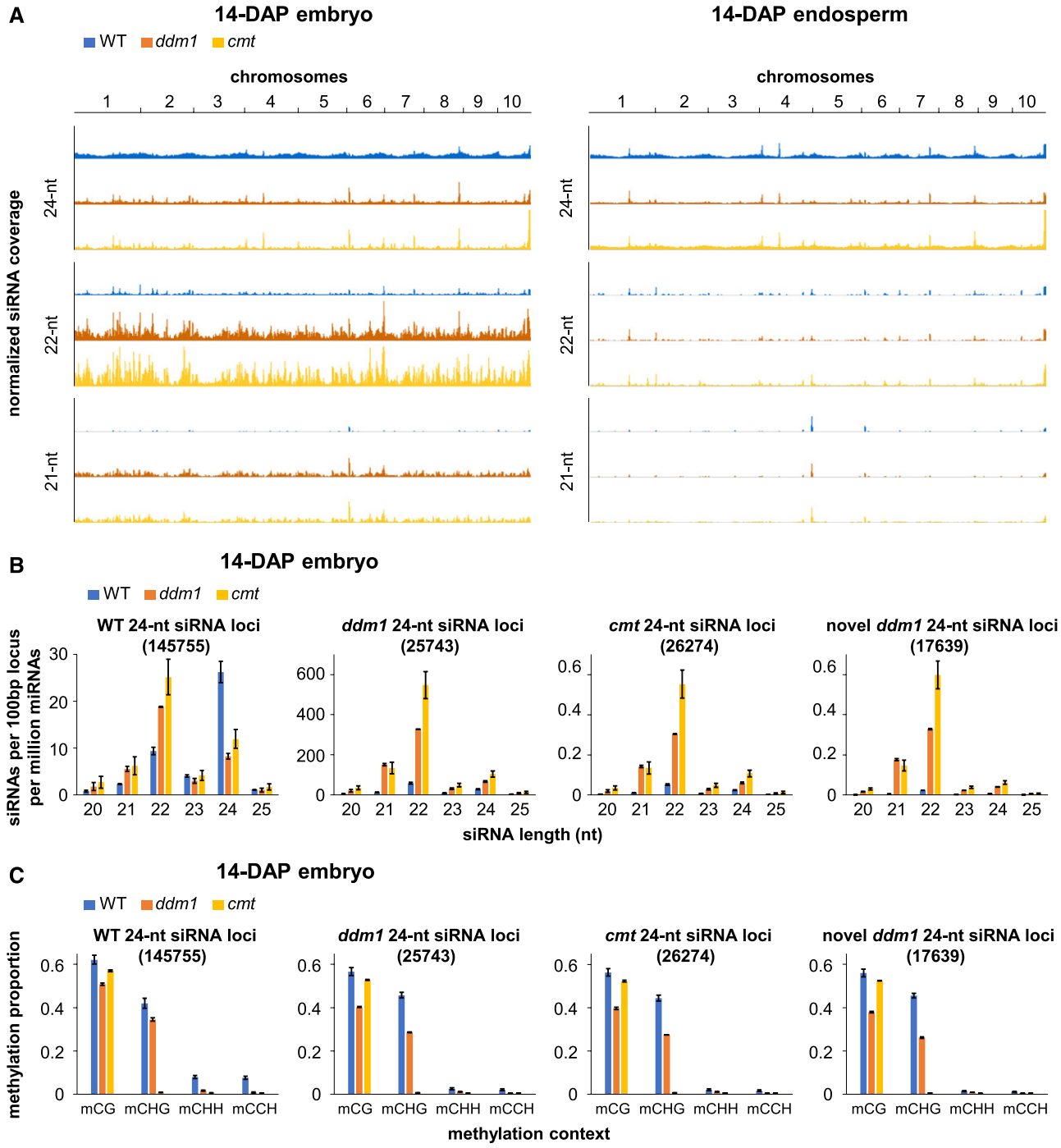

Figure 3. 24-Nucleotide siRNA Loci in Mutants.

(A) Whole-chromosome siRNA patterns. Average siRNA coverage on 5-Mb intervals (per 500,000 miRNAs) is shown for each of the 10 chromosomes for 14-DAP embryo and 14-DAP endosperm. Coverage is on the same scale in every track, with a maximum value of 0.4 overlapping siRNAs per base pair. The peaks are cut off at loci that exceed this value.

(B) siRNA lengths in 24-nucleotide siRNA loci in embryos. siRNA counts were normalized by miRNA count and by the number of loci in each set (shown in parentheses). All siRNAs that overlapped by at least half their lengths with each type of locus were included. Error bars are standard errors of the means for the biological replicates of each genotype.

(C) DNA methylation in 24-nucleotide siRNA loci in embryos. Average methylation for each set of loci was calculated as the proportion of methylated C over total C in each sequence context. Error bars are standard errors of the means for the biological replicates of each genotype.

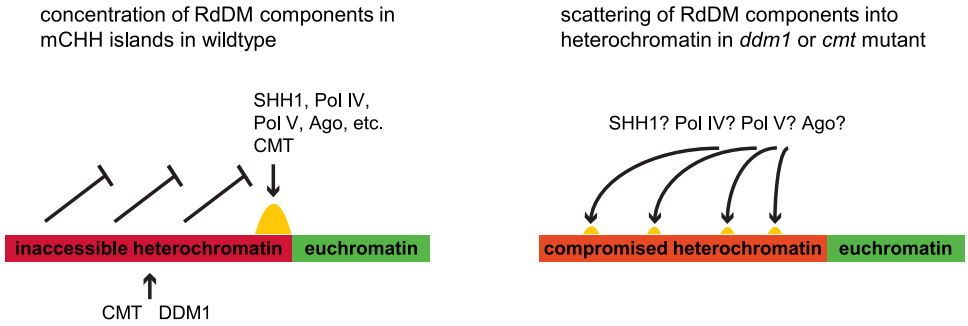

Figure 4. A Hypothetical Explanation for Loss of RdDM in *ddm1* and *cmt* Mutants.

In wild-type conditions, heterochromatin is maintained in an inaccessible state that excludes RdDM. All the components required for RdDM are then concentrated at a small set of loci in the genome (mCHH islands) where they function in concert to methylate DNA. In the absence of chromomethylases or DDM1-type nucleosome remodelers, heterochromatin no longer excludes RdDM, and RdDM components are scattered over a larger area of repetitive DNA.

Harbinger, *Mutator*, *hAT*, and *Mariner* superfamilies are enriched in mCHH islands (Gent et al., 2013). The 24-nucleotide siRNAs from these terminal inverted repeat (TIR) transposons were reduced ~8-fold in *cmt* and in *ddm1* (Figure 2D).

Gain of siRNAs in Heterochromatin in *cmt* and *ddm1*

Retrotransposons with long terminal repeats (LTRs), which are relatively depleted in mCHH islands but have high copy numbers elsewhere in maize heterochromatin, gained both 21- and 22-nucleotide siRNAs in the mutants (8.8-fold gain of 21-nucleotide siRNAs in *ddm1*, 7.0-fold gain of 21-nucleotide siRNAs in *cmt*- 4.6-fold gain of 22-nucleotide siRNAs in *ddm1*, and 6.2-fold gain of 22-nucleotide siRNAs in *cmt*; Figure 2D). We also examined siRNAs at two types of high-copy tandem repeats: centromeric *CentC* and noncentromeric *knob180*. Both types are depleted of mCHH and siRNAs in wild-type plants (Gent et al., 2012, 2014), but in the *ddm1* 14-DAP embryos, *knob180* produced 8-fold more 21-nucleotide siRNAs, 18-fold more 22-nucleotide siRNAs, and 6-fold more 24-nucleotide siRNAs than in the wild type (Figure 2D). This increase in *knob180* siRNAs was not accompanied by an increase in mCHH (Figure 2E). A chromosome-level view of 24-nucleotide siRNA coverage showed enrichment toward chromosome arms in wild-type 14-DAP endosperm and embryo, corresponding to gene density and mCHH islands, whereas 21- and 22-nucleotide siRNAs had a more uneven distribution with large numbers of siRNAs at discrete loci (Figure 3A). In *cmt* and *ddm1* 14-DAP embryos, 24-nucleotide siRNAs showed a distribution similar to wild-type 21- and 22-nucleotide siRNAs, with a strong reduction at the majority of loci across the genome. We split the genome into 100-bp bins and counted the number of 24-nucleotide siRNAs normalized per 500,000 miRNAs that overlapped each bin. We required that at least 14 bp of each siRNA overlap with the bin in order to be counted. Any locus with at least five overlapping siRNAs and with siRNAs spanning at least 50 of its 100 bp was defined as a 24-nucleotide siRNA locus. In wild-type 14-DAP embryos, 176,342 loci met these criteria, while only 26,519 did in *ddm1* embryos and 26,546 did in *cmt* embryos. We also identified the subset of 17,985 novel *ddm1* 24-nucleotide siRNAs that did not meet the criteria in the wild type. Despite the *ddm1* and *cmt* 24-nucleotide siRNA loci being defined solely by 24-nucleotide siRNAs, they were more strongly enriched for 21- and 22-nucleotide siRNAs than 24-nucleotide siRNAs (Figure 3B). Similar to the *knob180* tandem repeat (Figure 2E), the *cmt*, *ddm1*, and novel 24-nucleotide siRNA loci were highly methylated in mCG and mCHG and poorly methylated in mCHH in the wild type and did not gain mCHH in either mutant (Figure 3C).

DISCUSSION

We found that double mutants of the chromomethylases *zmet2* and *zmet5* (*cmt*) and double mutants of the DDM1-type nucleosome remodelers *chr101* and *chr106* (*ddm1*) were deficient in canonical RdDM, as indicated by loss of DNA methylation and 24-nucleotide siRNAs in mCHH islands. The near complete loss of mCHG in *cmt* is what would be expected for *mu1013094* and *mu1017456* being null alleles (Figures 1 and 3). The smaller reductions in mCHG/mCG in *ddm1* is consistent with null alleles of *ddm1* in Arabidopsis and rice (*Oryza sativa*; Zemach et al., 2013; Tan et al., 2016; Lyons and Zilberman, 2017), but in the absence of a clear expectation for a *ddm1* phenotype in maize, residual DDM1 activity in *mu1044815* or *mu1021319* is theoretically possible. The complete nonviability of the *ddm1* kernels indicates that the mutants are at least severe hypomorphs. What was unexpected for both *cmt* and *ddm1* was the near complete loss of RdDM. In 14-DAP embryos, methylation in the CHH context (mCHH) was more strongly reduced in *cmt* than in *ddm1*. The residual mCHH in *ddm1* could be explained by continued activity of ZMET2 and ZMET5, as the mCCH subcategory of mCHH, which is more strictly dependent on RdDM (Gouil and Baulcombe, 2016), was reduced to similar levels in both *ddm1* and *cmt* (Figure 1A). In maize, the effect of *cmt* and *ddm1* mutants was weaker in 14-DAP endosperm than in 14-DAP embryo and weaker than in mature endosperm. Transfer of wild-type maternal products directly into developing endosperm might explain these differences.

In agreement with loss of RdDM, 24-nucleotide siRNAs in embryos were reduced to nearly background levels in *ddm1* and in *cmt* in regions that had high levels of RdDM in the wild type (Figures 2 and 3). The corresponding gain of 21-, 22-, and 24-nucleotide siRNAs in heterochromatin, particularly in retrotransposons, is consistent with their increased siRNA and mRNA expression in *ddm1* mutants in Arabidopsis (Onodera et al., 2005; Creasey et al., 2014; McCue et al., 2015). The *knob180* tandem repeat in maize is associated with an extreme form of heterochromatin (Peacock et al., 1981). *knob180* siRNAs increased up to 18-fold in abundance in *ddm1* but not in *cmt* (Figure 2D). Even though 24-nucleotide siRNAs also increased, mCHH decreased, indicating that these siRNAs did not lead to productive RdDM. The fact that production of siRNAs requires transcription indicates transcriptional derepression of *knob180* in *ddm1* and suggests that DDM1-type nucleosome remodelers can have roles in transcriptional silencing independent of chromomethylation. The total number of 24-nucleotide siRNAs was only decreased to about half of wild-type levels relative to miRNAs (Figure 2B), and they were retained at high levels at discrete loci throughout the genome (Figure 3A). Loci that retained or gained 24-nucleotide siRNAs in *ddm1* or *cmt* embryos tended to have abundant 21- and 22-nucleotide siRNAs, even in the wild type (Figure 3B). In Arabidopsis, the additional siRNAs produced in *ddm1* mutants can direct mCHH using alternative forms of RdDM in developing flower buds, but not in leaves (Nuthikattu et al., 2013; McCue et al., 2015; Panda et al., 2016). In maize embryos, the loci that gained or retained 24-nucleotide siRNAs in *ddm1* and *cmt* embryos, and that were rich in 21- and 22-nucleotide siRNAs, had low mCHH in the wild type and even lower in mutants. This was true even for novel *ddm1* 24-nucleotide siRNA loci that did not qualify as 24-nucleotide siRNA loci in the wild type (Figure 3C).

De novo RdDM can initiate CMT activity (Jackel et al., 2016; Fultz and Slotkin, 2017), yet it appears that in maize CMT is required to maintain canonical RdDM. One explanation for loss of RdDM in the *cmt* mutant is that CMT produces mCHG, which leads to H3K9me2. In Arabidopsis, the H3K9me2 binding protein SAWADEE HOMEODOMAIN HOMOLOG1 (SHH1) recruits Pol IV (Law et al., 2013; Zhang et al., 2013). Maize SHH1 interacts with both the Pol IV and Pol V protein complexes (Haag et al., 2014). In addition, since chromomethylases can also produce mCHH (Gouil and Baulcombe, 2016), not all mCHH is dependent on RdDM even at loci that are undergoing RdDM. Some of the decrease in mCHH in *cmt* is a direct consequence of loss of CMT rather than a loss of RdDM. This is evident in 14-DAP embryos, where *cmt* had a more severe loss of mCHH than *ddm1* did (Figure 1A). The similarly strong loss of 24-nucleotide siRNAs in *cmt* and *ddm1* indicates that RdDM was similarly affected in both mutants.

However, the principle reason for loss of RdDM in *cmt* and *ddm1* may be simple dilution. The loss of methylation from heterochromatin could result in the spreading of at least one critical RdDM component from mCHH islands into the newly accessible heterochromatin (Figure 4). Rather than an increase in RdDM at new sites across the genome, we might expect a global decrease because no specific loci would reproducibly recruit the full complement of RdDM components needed to sustain sufficient DRM activity to keep up with the constant loss of methylation during DNA replication. The absence of mCHH in the genome in *ddm1* and *cmt* could be explained if even a single critical RdDM component were present at too low a concentration.

Three lines of evidence support the dilution hypothesis. First is the >50% loss of RdDM observed in single mutants of either *zmet2* or *zmet5* in leaf tissues (Supplemental Figure 4) (Li et al., 2015a). A mild increase in heterochromatin accessibility genome wide could have a large effect in diluting RdDM components from mCHH islands and exacerbate these single mutant phenotypes. The second is the loss of RdDM without the loss of mCHG in mCHH islands in *ddm1* mutants (Figure 1). This observation rules out the simple scenario that DDM1 is required for chromomethylation, which is then required for RdDM, and suggests an alternative explanation such as the RdDM dilution model. Finally, there is no evidence for DDM1 functioning directly in RdDM. Instead, nucleosome remodeling in each stage of RdDM is accomplished by distinct SNF2 family nucleosome remodelers: CLSY and DRD1 in Arabidopsis (Kanno et al., 2004; Smith et al., 2007) and CHR167 and RMR1 in maize (Hale et al., 2007; Haag et al., 2014). In contrast, an increase in heterochromatin accessibility to RdDM components genome wide in *ddm1* is strongly consistent with its known function and mutant phenotypes (Gendrel et al., 2002; Soppe et al., 2002; Onodera et al., 2005; Zemach et al., 2013; Creasey et al., 2014; McCue et al., 2015; Lyons and Zilberman, 2017).

The severity of the effect of *ddm1* and *cmt* mutants on RdDM may be related to genome size. RdDM in rice, with a genome one-quarter the size of maize, appears to have an intermediate dependence on *ddm1*: A double mutant of DDM1-type nucleosome remodelers in rice had an ~50% reduction in mCHH near genes and a slight increase in mCHH in regions not normally undergoing RdDM (Tan et al., 2016). In Arabidopsis, with a genome one-nineteenth the size of maize, there is minor loss of mCHH from RdDM loci in a *ddm1* mutant (as indicated by analysis of differentially methylated regions; Stroud et al., 2013) and substantial loss of 24-nucleotide siRNA from many non-LTR transposons (Creasey et al., 2014). It is possible that loss of RdDM in Arabidopsis mutants that lack H3K9me2 might be partially explained by the dilution model rather than simply by direct involvement of H3K9me2 in RdDM (Stroud et al., 2014). If so, Arabidopsis H3K9 methyltransferase mutants or *cmt* mutants (particularly *cmt* triple mutants) would also be expected to exhibit increased siRNA production in heterochromatin, as has been demonstrated with *ddm1* (Onodera et al., 2005; Creasey et al., 2014; McCue et al., 2015). We look forward to learning whether the dilution model for loss of RdDM in *ddm1* and *cmt* holds true not only in maize, but also as a general feature of plant genomes. What is clear from our data, however, is that both DDM1 and CMT are required for canonical RdDM in maize, and in their absence, siRNAs of multiple lengths are produced in normally heterochromatic regions.

METHODS

Plant Materials and Plant Growth Conditions

PCR primers, alleles, and gene names for all *ddm1* and *cmt* mutants used in this study are listed in Supplemental Table 1, including published

zmet alleles (Li et al., 2014). Primers for *mop1-1* genotyping are as published previously (Madzima et al., 2014). Wild-type controls for *ddm1* and *cmt* were derivatives of the same UniformMu lineage carrying the *ddm1 Mu* insertions *mu1044815* and *mu1021319* and were progeny of homozygous wild-type parents. Wild-type controls for *mop1-1* were homozygous *Mop1* siblings of the homozygous *mop1-1* mutants in the B73 background (derived from Madzima et al. [2014], but further introgressed into B73 another generation).

Developing endosperm and embryos were collected 14 DAP and flash-frozen in liquid nitrogen for later nucleic acid extraction. Prior to freezing, pericarps were removed from kernels and the embryos separated from the endosperm. The parent plants were grown in a winter greenhouse with supplemental lighting from high pressure sodium bulbs for 14 h a day. Each endosperm was cut into two halves, one for DNA extraction and one for RNA extraction. Genotypes of embryos were inferred by genotyping of endosperm. For mature endosperm, dry kernels were soaked in 6% NaOH in water at 57°C for 8 min and the embryos and pericarps removed with forceps. Each mature endosperm was ground to a powder with a mortar and pestle. Frozen 14-DAP endosperms and embryos were ground with micropestles in 2-mL microcentrifuge tubes without thawing. DNA was extracted from all three tissue types, each individual sample separately, with the DNeasy Plant Mini Kit (Qiagen; no. 69104).

WGBS and Small RNA Sequencing

WGBS libraries were prepared using the methylC-seq method (Urich et al., 2015) with no more than seven cycles of PCR amplification for endosperm and no more than 10 for embryo. For the mature endosperm libraries of Figure 1C, DNA from three individuals was combined. For all other libraries, separate libraries were made from each individual embryo or endosperm. All results shown are the average of two to four individuals per genotype, except *Zmet2/zmet2 zmet5/zmet5* in Supplemental Figure 2, which is derived from a single embryo.

RNA was extracted from individual 14-DAP embryos and 14-DAP endosperm using mirVana miRNA isolation kits (Thermo Fisher Scientific; no. AM1560) using the total RNA method. For the 14-DAP endosperm, Plant RNA Isolation Aid (Thermo Fisher Scientific; no. AM9690) was added at the lysis step. Small RNA sequencing libraries were prepared from individual embryos and endosperm (two or three for each genotype) using the NEXTflex Small RNA-Seq Kit v3 (Bioo Scientific; no. 5132-05) with 13 cycles of PCR amplification for endosperm and 17 cycles for embryo. The 150-nucleotide single-end Illumina sequencing was performed on an Illumina NextSeq 500 system at the Georgia Genomics Facility, University of Georgia.

BS-seq reads were trimmed and quality filtered using cutadapt (version 1.9.dev1 with Python 2.7.8) (Martin, 2011), command line parameters "-q 20 -a AGATCGGAAGAGC -e .1 -O 1 -m 50." Trimmed reads were aligned to the B73 RefGen_v4 maize genome (Jiao et al., 2017) using BS-Seeker2 (v2.1.1 with Python 2.7.8 and Bowtie2 2.2.9) with default parameters except –m 1 to allow for a single mismatch. All libraries were aligned to the *Zea* consensus sequences of the 156-bp tandem repeat *CentC* and the 180-bp tandem repeat *knob180* (Gent et al., 2017) using BS-seeker2 in the same way, except up to four mismatches were allowed per read.

Small RNA-seq reads were trimmed and quality filtered using cutadapt (version 1.14 with Python 2.7.8) (Martin, 2011), command line parameters "-u 4 -q 20 -a TGGAATTCTCGGGTGCCAAGG -e .05 -O 20 --discard-untrimmed -m 24 -M 29," followed by a second trim with just "-u -4." In this way adapter sequences and the four random nucleotides at each end of each RNA were trimmed and all reads outside the range of 20 to 25 nucleotides were removed. NCBI BLAST (version 2.2.26) was used to identify reads corresponding to the set of maize mature miRNA sequences from miRBase (version 20; Kozomara and Griffiths-Jones, 2011). The blastall Expectation value was set to 1e-5. Reads corresponding to the tandem repeats *CentC* and *knob180* (Gent et al., 2017) were identified similarly, except the blastall Expectation value was set to 1e-6. The consensus sequence for each was turned into a dimer to allow reads that spanned the junctions between monomers to be identified. After removing all identified miRNAs from the small RNA reads, the remaining 20- to 25-nucleotide reads were mapped to the B73 RefGen_v4 maize genome (Jiao et al., 2017) using BWA-backtrack (version 0.7.15; Li and Durbin, 2009), command line parameters "aln -t 8 -l 10." All mapping reads were included in the set of siRNAs, including nonuniquely mapping reads, except in the analyses of Figures 2B and 2C, where the subset of uniquely mapping siRNAs were identified based on MAPQ values of at least 20. All results shown are averages from two or three individual embryos or endosperms. Whole-genome coverage was calculated on 5-Mb intervals and visualized using the Integrative Genomics Viewer (Thorvaldsdóttir et al., 2013).

Accession Numbers

All sequencing reads have been deposited in the Sequence Read Archive under accession number SRP127627. Read counts for each experiment and SRA accession numbers are listed in Supplemental Tables 4 and 5. Alleles and gene IDs are listed in Supplemental Table 1.

Supplemental Data

Supplemental Figure 1. Pigment sectoring and small embryo phenotypes of double mutant kernels.

Supplemental Figure 2. DNA methylation in 14-DAP embryos of *zmet2 zmet5* heterozygote and homozygote combinations.

Supplemental Figure 3. DNA methylation in mature endosperm of *chr101 chr106* heterozygote and homozygote combinations.

Supplemental Figure 4. DNA methylation in leaves and developing ears of single mutants of *zmet2-m1* and *zmet5-m1*.

Supplemental Table 1. Mutant alleles and genotyping primers.

Supplemental Table 2. Kernel genotypes and phenotypes.

Supplemental Table 3. Segregation of *zmet2* and *zmet5* alleles and *chr101* and *chr106* alleles.

Supplemental Table 4. Whole-genome bisulfite sequencing libraries.

Supplemental Table 5. Small RNA sequencing libraries.

ACKNOWLEDGMENTS

We thank Sean Trostel for assistance with genotyping, the Maize Genetics Cooperation Stock Center for providing UniformMu stocks, and Nathan Springer for providing other stocks and for comments on the manuscript. This study was supported in part by resources and technical expertise from the Georgia Advanced Computing Resource Center, a partnership between the University of Georgia's Office of the Vice President for Research and Office of the Vice President for Information Technology. Funding for this study was provided by the National Science Foundation (0922703 and 1118550 to R.K.D. and 1547760 to J.I.G.).

AUTHOR CONTRIBUTIONS

F.-F.F. designed and performed research. R.K.D. designed research and wrote the article. J.I.G. designed and performed research, analyzed data, and wrote the article.

Received January 23, 2018; revised May 16, 2018; accepted June 7, 2018; published June 8, 2018.

REFERENCES

Bewick, A.J., Niederhuth, C.E., Ji, L., Rohr, N.A., Griffin, P.T., Leebens-Mack, J., and Schmitz, R.J. (2017). The evolution of CHROMOMETHYLASES and gene body DNA methylation in plants. Genome Biol. **18:** 65.

Blevins, T., Pontvianne, F., Cocklin, R., Podicheti, R., Chandrasekhara, C., Yerneni, S., Braun, C., Lee, B., Rusch, D., Mockaitis, K., Tang, H., and Pikaard, C.S. (2014). A two-step process for epigenetic inheritance in Arabidopsis. Mol. Cell **54:** 30–42.

Calarco, J.P., Borges, F., Donoghue, M.T., Van Ex, F., Jullien, P.E., Lopes, T., Gardner, R., Berger, F., Feijó, J.A., Becker, J.D., and Martienssen, R.A. (2012). Reprogramming of DNA methylation in pollen guides epigenetic inheritance via small RNA. Cell **151:** 194–205.

Creasey, K.M., Zhai, J., Borges, F., Van Ex, F., Regulski, M., Meyers, B.C., and Martienssen, R.A. (2014). miRNAs trigger widespread epigenetically activated siRNAs from transposons in Arabidopsis. Nature **508:** 411–415.

Cuerda-Gil, D., and Slotkin, R.K. (2016). Non-canonical RNA-directed DNA methylation. Nat. Plants **2:** 16163.

Dennis, K., Fan, T., Geiman, T., Yan, Q., and Muegge, K. (2001). Lsh, a member of the SNF2 family, is required for genome-wide methylation. Genes Dev. **15:** 2940–2944.

Du, J., Johnson, L.M., Jacobsen, S.E., and Patel, D.J. (2015). DNA methylation pathways and their crosstalk with histone methylation. Nat. Rev. Mol. Cell Biol. **16:** 519–532.

Fultz, D., and Slotkin, R.K. (2017). Exogenous transposable elements circumvent identity-based silencing, permitting the dissection of expression-dependent silencing. Plant Cell **29:** 360–376.

Gao, Z., et al. (2010). An RNA polymerase II- and AGO4-associated protein acts in RNA-directed DNA methylation. Nature **465:** 106–109.

Gendrel, A.V., Lippman, Z., Yordan, C., Colot, V., and Martienssen, R.A. (2002). Dependence of heterochromatic histone H3 methylation patterns on the Arabidopsis gene DDM1. Science **297:** 1871–1873.

Gent, J.I., Dong, Y., Jiang, J., and Dawe, R.K. (2012). Strong epigenetic similarity between maize centromeric and pericentromeric regions at the level of small RNAs, DNA methylation and H3 chromatin modifications. Nucleic Acids Res. **40:** 1550–1560.

Gent, J.I., Ellis, N.A., Guo, L., Harkess, A.E., Yao, Y., Zhang, X., and Dawe, R.K. (2013). CHH islands: de novo DNA methylation in near-gene chromatin regulation in maize. Genome Res. **23:** 628–637.

Gent, J.I., Madzima, T.F., Bader, R., Kent, M.R., Zhang, X., Stam, M., McGinnis, K.M., and Dawe, R.K. (2014). Accessible DNA and relative depletion of H3K9me2 at maize loci undergoing RNA-directed DNA methylation. Plant Cell **26:** 4903–4917.

Gent, J.I., Wang, N., and Dawe, R.K. (2017). Stable centromere positioning in diverse sequence contexts of complex and satellite centromeres of maize and wild relatives. Genome Biol. **18:** 121.

Gouil, Q., and Baulcombe, D.C. (2016). DNA methylation signatures of the plant chromomethyltransferases. PLoS Genet. **12:** e1006526.

Greenberg, M.V., Deleris, A., Hale, C.J., Liu, A., Feng, S., and Jacobsen, S.E. (2013). Interplay between active chromatin marks and RNA-directed DNA methylation in *Arabidopsis thaliana*. PLoS Genet. **9:** e1003946.

Haag, J.R., et al. (2014). Functional diversification of maize RNA polymerase IV and V subtypes via alternative catalytic subunits. Cell Reports **9:** 378–390.

Hale, C.J., Stonaker, J.L., Gross, S.M., and Hollick, J.B. (2007). A novel Snf2 protein maintains trans-generational regulatory states established by paramutation in maize. PLoS Biol. **5:** e275.

Hollick, J.B. (2017). Paramutation and related phenomena in diverse species. Nat. Rev. Genet. **18:** 5–23.

Holoch, D., and Moazed, D. (2015). RNA-mediated epigenetic regulation of gene expression. Nat. Rev. Genet. **16:** 71–84.

Hsieh, P.H., He, S., Buttress, T., Gao, H., Couchman, M., Fischer, R.L., Zilberman, D., and Feng, X. (2016). Arabidopsis male sexual lineage exhibits more robust maintenance of CG methylation than somatic tissues. Proc. Natl. Acad. Sci. USA **113:** 15132–15137.

Ibarra, C.A., et al. (2012). Active DNA demethylation in plant companion cells reinforces transposon methylation in gametes. Science **337:** 1360–1364.

Jackel, J.N., Storer, J.M., Coursey, T., and Bisaro, D.M. (2016). Arabidopsis RNA polymerases IV and V are required to establish H3K9 methylation, but not cytosine methylation, on geminivirus chromatin. J. Virol. **90:** 7529–7540.

Jiao, Y., et al. (2017). Improved maize reference genome with single-molecule technologies. Nature **546:** 524–527.

Johnson, C., Kasprzewska, A., Tennessen, K., Fernandes, J., Nan, G.L., Walbot, V., Sundaresan, V., Vance, V., and Bowman, L.H. (2009). Clusters and superclusters of phased small RNAs in the developing inflorescence of rice. Genome Res. **19:** 1429–1440.

Johnson, L.M., Law, J.A., Khattar, A., Henderson, I.R., and Jacobsen, S.E. (2008). SRA-domain proteins required for DRM2-mediated de novo DNA methylation. PLoS Genet. **4:** e1000280.

Johnson, L.M., Du, J., Hale, C.J., Bischof, S., Feng, S., Chodavarapu, R.K., Zhong, X., Marson, G., Pellegrini, M., Segal, D.J., Patel, D.J., and Jacobsen, S.E. (2014). SRA- and SET-domain-containing proteins link RNA polymerase V occupancy to DNA methylation. Nature **507:** 124–128.

Kanno, T., Mette, M.F., Kreil, D.P., Aufsatz, W., Matzke, M., and Matzke, A.J. (2004). Involvement of putative SNF2 chromatin remodeling protein DRD1 in RNA-directed DNA methylation. Curr. Biol. **14:** 801–805.

Kozomara, A., and Griffiths-Jones, S. (2011). miRBase: integrating microRNA annotation and deep-sequencing data. Nucleic Acids Res. **39:** D152–D157.

Kuhlmann, M., and Mette, M.F. (2012). Developmentally non-redundant SET domain proteins SUVH2 and SUVH9 are required for transcriptional gene silencing in Arabidopsis thaliana. Plant Mol. Biol. **79:** 623–633.

Law, J.A., Du, J., Hale, C.J., Feng, S., Krajewski, K., Palanca, A.M., Strahl, B.D., Patel, D.J., and Jacobsen, S.E. (2013). Polymerase IV occupancy at RNA-directed DNA methylation sites requires SHH1. Nature **498:** 385–389.

Lee, T.F., Gurazada, S.G., Zhai, J., Li, S., Simon, S.A., Matzke, M.A., Chen, X., and Meyers, B.C. (2012). RNA polymerase V-dependent small RNAs in Arabidopsis originate from small, intergenic loci including most SINE repeats. Epigenetics **7:** 781–795.

Li, Q., et al. (2014). Genetic perturbation of the maize methylome. Plant Cell **26:** 4602–4616.

Li, Q., et al. (2015a). RNA-directed DNA methylation enforces boundaries between heterochromatin and euchromatin in the maize genome. Proc. Natl. Acad. Sci. USA **112:** 14728–14733.

Li, H., and Durbin, R. (2009). Fast and accurate short read alignment with Burrows-Wheeler transform. Bioinformatics **25:** 1754–1760.

Li, S., Vandivier, L.E., Tu, B., Gao, L., Won, S.Y., Li, S., Zheng, B., Gregory, B.D., and Chen, X. (2015b). Detection of Pol IV/RDR2-dependent transcripts at the genomic scale in Arabidopsis reveals features and regulation of siRNA biogenesis. Genome Res. **25:** 235–245.

Liu, Z.W., Shao, C.R., Zhang, C.J., Zhou, J.X., Zhang, S.W., Li, L., Chen, S., Huang, H.W., Cai, T., and He, X.J. (2014). The SET domain proteins SUVH2 and SUVH9 are required for Pol V occupancy at RNA-directed DNA methylation loci. PLoS Genet. **10:** e1003948.

Lyons, D.B., and Zilberman, D. (2017). DDM1 and Lsh remodelers allow methylation of DNA wrapped in nucleosomes. eLife **6:** e30674.

Madzima, T.F., Huang, J., and McGinnis, K.M. (2014). Chromatin structure and gene expression changes associated with loss of MOP1 activity in *Zea mays*. Epigenetics **9:** 1047–1059.

Martin, M. (2011). Cutadapt removes adapter sequences from high-throughput sequencing reads. EMBnet J. **17:** 3.

McCarty, D.R., et al. (2005). Steady-state transposon mutagenesis in inbred maize. Plant J. **44:** 52–61.

McCue, A.D., Panda, K., Nuthikattu, S., Choudury, S.G., Thomas, E.N., and Slotkin, R.K. (2015). ARGONAUTE 6 bridges transposable element mRNA-derived siRNAs to the establishment of DNA methylation. EMBO J. **34:** 20–35.

Mérai, Z., et al. (2014). The AAA-ATPase molecular chaperone Cdc48/p97 disassembles sumoylated centromeres, decondenses heterochromatin, and activates ribosomal RNA genes. Proc. Natl. Acad. Sci. USA **111:** 16166–16171.

Niederhuth, C.E., et al. (2016). Widespread natural variation of DNA methylation within angiosperms. Genome Biol. **17:** 194.

Nobuta, K., et al. (2008). Distinct size distribution of endogeneous siRNAs in maize: Evidence from deep sequencing in the mop1-1 mutant. Proc. Natl. Acad. Sci. USA **105:** 14958–14963.

Nuthikattu, S., McCue, A.D., Panda, K., Fultz, D., DeFraia, C., Thomas, E.N., and Slotkin, R.K. (2013). The initiation of epigenetic silencing of active transposable elements is triggered by RDR6 and 21-22 nucleotide small interfering RNAs. Plant Physiol. **162:** 116–131.

Onodera, Y., Haag, J.R., Ream, T., Costa Nunes, P., Pontes, O., and Pikaard, C.S. (2005). Plant nuclear RNA polymerase IV mediates siRNA and DNA methylation-dependent heterochromatin formation. Cell **120:** 613–622.

Panda, K., Ji, L., Neumann, D.A., Daron, J., Schmitz, R.J., and Slotkin, R.K. (2016). Full-length autonomous transposable elements are preferentially targeted by expression-dependent forms of RNA-directed DNA methylation. Genome Biol. **17:** 170.

Peacock, W.J., Dennis, E.S., Rhoades, M.M., and Pryor, A.J. (1981). Highly repeated DNA sequence limited to knob heterochromatin in maize. Proc. Natl. Acad. Sci. USA **78:** 4490–4494.

Rowley, M.J., Rothi, M.H., Böhmdorfer, G., Kuciński, J., and Wierzbicki, A.T. (2017). Long-range control of gene expression via RNA-directed DNA methylation. PLoS Genet. **13:** e1006749.

Satyaki, P.R., and Gehring, M. (2017). DNA methylation and imprinting in plants: machinery and mechanisms. Crit. Rev. Biochem. Mol. Biol. **52:** 163–175.

Schoft, V.K., Chumak, N., Mosiolek, M., Slusarz, L., Komnenovic, V., Brownfield, L., Twell, D., Kakutani, T., and Tamaru, H. (2009). Induction of RNA-directed DNA methylation upon decondensation of constitutive heterochromatin. EMBO Rep. **10:** 1015–1021.

Sekhon, R.S., Lin, H., Childs, K.L., Hansey, C.N., Buell, C.R., de Leon, N., and Kaeppler, S.M. (2011). Genome-wide atlas of transcription during maize development. Plant J. **66:** 553–563.

Slotkin, R.K., Vaughn, M., Borges, F., Tanurdzić, M., Becker, J.D., Feijó, J.A., and Martienssen, R.A. (2009). Epigenetic reprogramming and small RNA silencing of transposable elements in pollen. Cell **136:** 461–472.

Smith, L.M., Pontes, O., Searle, I., Yelina, N., Yousafzai, F.K., Herr, A.J., Pikaard, C.S., and Baulcombe, D.C. (2007). An SNF2 protein associated with nuclear RNA silencing and the spread of a silencing signal between cells in Arabidopsis. Plant Cell **19:** 1507–1521.

Soppe, W.J., Jasencakova, Z., Houben, A., Kakutani, T., Meister, A., Huang, M.S., Jacobsen, S.E., Schubert, I., and Fransz, P.F. (2002). DNA methylation controls histone H3 lysine 9 methylation and heterochromatin assembly in Arabidopsis. EMBO J. **21:** 6549–6559.

Stroud, H., Greenberg, M.V., Feng, S., Bernatavichute, Y.V., and Jacobsen, S.E. (2013). Comprehensive analysis of silencing mutants reveals complex regulation of the Arabidopsis methylome. Cell **152:** 352–364.

Stroud, H., Do, T., Du, J., Zhong, X., Feng, S., Johnson, L., Patel, D.J., and Jacobsen, S.E. (2014). Non-CG methylation patterns shape the epigenetic landscape in Arabidopsis. Nat. Struct. Mol. Biol. **21:** 64–72.

Tan, F., Zhou, C., Zhou, Q., Zhou, S., Yang, W., Zhao, Y., Li, G., and Zhou, D.X. (2016). Analysis of chromatin regulators reveals specific features of rice DNA methylation pathways. Plant Physiol. **171:** 2041–2054.

Thorvaldsdóttir, H., Robinson, J.T., and Mesirov, J.P. (2013). Integrative Genomics Viewer (IGV): high-performance genomics data visualization and exploration. Brief. Bioinform. **14:** 178–192.

Urich, M.A., Nery, J.R., Lister, R., Schmitz, R.J., and Ecker, J.R. (2015). MethylC-seq library preparation for base-resolution whole-genome bisulfite sequencing. Nat. Protoc. **10:** 475–483.

Wang, X., Elling, A.A., Li, X., Li, N., Peng, Z., He, G., Sun, H., Qi, Y., Liu, X.S., and Deng, X.W. (2009). Genome-wide and organ-specific landscapes of epigenetic modifications and their relationships to mRNA and small RNA transcriptomes in maize. Plant Cell **21:** 1053–1069.

Wassenegger, M., Heimes, S., Riedel, L., and Sänger, H.L. (1994). RNA-directed de novo methylation of genomic sequences in plants. Cell **76:** 567–576.

Woodhouse, M.R., Freeling, M., and Lisch, D. (2006). The mop1 (mediator of paramutation1) mutant progressively reactivates one of the two genes encoded by the MuDR transposon in maize. Genetics **172:** 579–592.

Zemach, A., Kim, M.Y., Hsieh, P.H., Coleman-Derr, D., Eshed-Williams, L., Thao, K., Harmer, S.L., and Zilberman, D. (2013). The Arabidopsis nucleosome remodeler DDM1 allows DNA methyltransferases to access H1-containing heterochromatin. Cell **153:** 193–205.

Zhai, J., Zhang, H., Arikit, S., Huang, K., Nan, G.L., Walbot, V., and Meyers, B.C. (2015). Spatiotemporally dynamic, cell-type-dependent premeiotic and meiotic phasiRNAs in maize anthers. Proc. Natl. Acad. Sci. USA **112:** 3146–3151.

Zhang, H., et al. (2013). DTF1 is a core component of RNA-directed DNA methylation and may assist in the recruitment of Pol IV. Proc. Natl. Acad. Sci. USA **110:** 8290–8295.

Zhong, X., Hale, C.J., Law, J.A., Johnson, L.M., Feng, S., Tu, A., and Jacobsen, S.E. (2012). DDR complex facilitates global association of RNA polymerase V to promoters and evolutionarily young transposons. Nat. Struct. Mol. Biol. **19:** 870–875.

Zhong, X., Du, J., Hale, C.J., Gallego-Bartolome, J., Feng, S., Vashisht, A.A., Chory, J., Wohlschlegel, J.A., Patel, D.J., and Jacobsen, S.E. (2014). Molecular mechanism of action of plant DRM de novo DNA methyltransferases. Cell **157:** 1050–1060.